PNC TN941 78−42

Sodium Mists Behavior in Cover Gas Space of an LMFBR

- Experimental Study -

March, 1978

POWER REACTOR AND NUCLEAR FUEL DEVELOPMENT CORPORATION

動力炉・核燃料開発事業団 (Power Reactor and Nuclear Fuel Development Corporation)

PNC TN941 78－42

Feb., 1978

Sodium Mists Behavior in Cover Gas Space of an LMFBR

- Experimental Study -

Y. Himeno* and J. Takahashi*

Abstract

This paper present the sodium mist behavor in Argon cover gas space of an LMFBR experimentaly using a test vessel of 1,400 mm in axial length, 305.5 mm in inner diameter and about 100 ℓ in volume. Experiments are consisted with measurements of the mist concentration and the mist gravitational settling flux between the sodium pool temperature range of 290° to 520°C. The results are discussed under the monosize assumption of the particles, and the particle sizes and evaporation rate are derived. Transient and steady state mist concentration behavior were also investigated.

KEYWORDS : LMFBR, sodium mist, aerosol, mist trap, laser scattering, in-situ measurement, settling mass flux, evaporation, nucleation theory, particle size, coagulation.

---

* Power Reactor and Nuclear Fuel Development Corporation, O-arai Engineering Center.

* Narita-cho, O-arai-machi, Ibaraki-pref.,

Contents

I. Introduction

In recent years, the knowledge on sodium mists behavior in cover gas space of an LMFBR has become increasingly important. This is an essential item for evaluation of the vapor deposition onto cooled annular walls of the reactor components as was suggested in the previous study[1] by the first author of this paper.

However the works related to this are very limited and this situation makes us difficult to design the components completely free from operational difficulties due to the vapor deposition. Accurate knowledge on the mist properties is also necessary for a mist trap (ie. vapor trap) design which has not yet been established to date.

With equal importance, the knowledge on evaporation rate of the vapor is necessary for deposition rate determination. Since, the mist are a kind of aerosols and, as is obvious from many previous studies on sodium-oxide aerosols[2] [3], the properties such as particle sizes and mass concentration of aerosols are very sensitive to their source rate.

II. Experimental Arrangement and Method

As the detailed explanation of the sodium loop used for the experiment has already been given in the previous paper[1], only the vessel geometry will be given in this paper with the arrangement of the experimental apparatuses.

1. Test Vessel

Fig. 1 shows the drawing of the test vessel. This vessel was already used in the previous experiment with the annuli test assemblies[1], and is 1,800mm in axial length and 305.5 mm in inner diameter. The circumference of the vessel is covered with thermal insulator and trace heaters, except its top flange.

Purified sodium of plugging temperature of 150°C or lower is feeded into the vessel from its bottom inlet so that the bottom about 400 mm depth is filled with sodium. Hight of the cover gas space above the pool is about 1,400 mm, and the cover gas volume is about 100 litters.

For the temperature measurement of the pool, cover gas and top wall surface of the vessel, thermocouples are arranged. Small flanges seen in Fig. 1 at the middle of the vessel are for the mists concentration determination by using of a laser scattering concentration meter and for the mists gravitational settling mass flux determination by using of the collection plates.

2. Absolute Method of Mists Concentration Determination

Cover gas flow sheets shown in Figs. 2 and 3 are for the mists concentration determination by mean of absolute method using filters. In these, mists trap, a back-up filter and an accumulated gas flow meter are installed. The mists traps are for mists collection by passing the cover gas through them. One mists trap shown in Fig. 2 is installed into the gas piping at the down stream position from the vessel, and the other one shown in Fig. 3 is installed into the cover gas space. The former trap is consisted with sintered stainless steel filters and the latter one is with stainless steel mesh. The back-up filters are for further collection of the mists which could not be removed by the traps. Experimentaly determined efficiencies of these two traps are 98% as shown in Fig. 4, and the efficiencies do not depend on their inlet mists concentration. These efficiencies were determined by using of the back-up filters.

Object of using two mist traps at different locations came from the requirement to investigate the supersaturation of the vapor within the cover gas. If, there existed large supersaturation, the concentration determined by these two traps may differe.

In the case of mists collection with the traps, the cover gas of the vessel was exhaused into the gas piping or the mist trap with very small flow rates of 2 to 6 ℓ/min. The mist trap located at the outside of the vessel seen in Fig. 2 has been preheated up to about 200°C prior to the collection. Inlet piping of this line has also been preheated up to the average cover gas temperature in the vessel to prevent the mists deposition onto the pipe wall.

During these cover gas exhausting, the purified Argon gas preheated up to the average cover gas temperature has been continueously feeded into the vessel so that the cover gas pressure could be kept constant. Purified Argon was prepared by passing 99.99% pure gas through the innert gas purification apparatus made of Plutinum and Paradium alloy. This apparatus was manufactured by Japan Pure Hydrogen Company, and the nominal purity of the gas produced by the apparatus is seven-nien.

Mists concentration was determined by measuring the collected sodium weight on the trap and accumulated volume of the gas which passed through the trap.

3. Relative Method of Mists Concentration Determination by Laser Scattering Meter.

As is well known, the laser beam is one of the most excellent light source for aerosol concentration and their particle size determinations[4]. This is because its power density is high and its wave length is monochromatic. Especially, the sodium mists concentration meter by using of laser has many good points. For example, windows for incoming and scattered beam can be made to be very small without complex divices such as focusing renses. These provide us to make the concentration meter with much reduced difficulties due to the vapor deposition onto the windows. In-site measurements of the concentration is also possible.

Fig. 5 shows the meter developed for the present experiment. Three pyrex glass windows, which are attached at the vessel side wall with the degree of 0, 90 and 180^0, are for the incoming (ie. primary), scattered and outgoing beam, respectively. Window for the outgoing beam is made in the form of light trap so that reflection of incoming beam can be prevented. Photodetector is attached at the window with 90° against the incoming beam.

Instrumentation and the beam source equipments of the meter is consisted with He-Ne laser source (wave length; 0.6328 μ m) of 20 mW made by NEC, a chopper (ratate with 225 Hz), a photodetector, a lock-in amplifier and a recorder. A synchroscope is for the adjustment of the lock-in amplifier. The reason of using a He-Ne laser beam came from the requirement to prevent large variation in the scattering cross-section of the particles due to particle size changing. With He-Ne laser beam of about 0.6 μ m wave length, the particle size parameter of α become to about 15 to 150, when the mist particle sizes are between 1.5 to 15 μ m as presented latter, and with these α, the scattering cross section does not so strongly depend on particle size[5].

The meter was calibrated prior its application to the test vessel by the above mentioned absolute method with the mist trap. Thereafter, it was used to in-situ concentration determination. The meter was also used for the particle size determination under limited conditions as will be give latter.

Fig. 6 shows the calibration data. The correlation between the scattering intensity and the concentration is quite satisfactory.

4. Determination Method of Gravitational Settling Mass Flux

The apparatus used for this determination is shown in Fig. 7. It is consisted with square windows faced upward, collection plates and handling arm. In the case of the flux determination, the apparatus was attached to the above mentioned window for the concentration meter by removing its glass window. Settling mists were collected for a certain period such as 10 to 50 hours onto the plates exposing then to the cover gas. Then, collected sodium mists was recovered. Settling mass flux were determined from the collected sodium weight, the surface area of the plates and the settling duration time.

III. Results and Discussion

1. Pool Temperature Dependence of Mists Concentration and Settling Mass Flux.

The concentration data of C determined by the absolute method with the mist traps and by the relative method with the laser concentration meter are presented in Fig. 8 with the settling mass flux data of ϕ_{sett} as a function of the saturated vapor pressure P_s at the pool surface. The top flange of the test vessel has been controlled to be 110° to 120°C during these measurements.

In Fig. 8, it can be seen that the agreement of the concentration data determined by the absolute and by the relative methods is quite well. It is also known that there is no large supersaturation of vapor within the cover gas. The concentration C and the settling mass flux ϕ_{sett} is seen to depend strongly on P_s. But, between T_s of 290° to 350°C, these two quantities are independent on P_s and are almost constant. At the higher T_s than these, P_s dependence of C changes at about 420°C. The concentration of C between T_s of 350° to 520° C are seen to be so large as 1.5×10^{-7} to 1.5×10^{-5} g/cm^3 (ie. 0.15 to 15 g/m^3).

These high concentration may probably caused by mist formation at the temperature coundary layer above the pool surface.

Causes of the change in C dependence on T_s at 290°, 350° and 420°C could not be made clear. Despite the difference in the cover gas geometery, the similar change in deposition rate of the vapor was also measured (at T_s of 420°C) in the previous experiment[1]. This suggests that the change in cover gas natural convection pattern may not be cause of these changes. Most probable cause of the change at 420°C may be the effect of hydrogen impurity in cover gas. Since, the hydrogen form sodium-hydride below about 420°C at atomospheric pressure, and it is likely that the hydride act as nucleus for mist formation.

2. Pool Temperature Dependence of the Evaporation Rate.

Although, vapor deposition rate onto the entire wall surface of the present cover gas space is not measured, it could be possible to estimate from the previous experiment with the annuli test assemblies[1] that about 85 %of the evaporated vapor rain back to the pool surface again and the rest about 15% of them deposited onto the wall.

If, it is assumed that the same fraction of the evaporated vapor were also deposited onto the present cover gas space wall, 1.18 times of the measured settling mass flux become equal to evaporation rate.

Fig. 9 shows thus obtained evaporation rate ϕ_e as a function of P_s. Since the deposition rate data below T_s of 400°C have not been determined in the previous experiment, ϕ_e below this temperature are not plotted in Fig. 9. The experimental evaporation rates by Kumada et al with natural and forced cover gas convections[6] and by Sutherland et al with natural cover gas convection[7] are also plotted in this Fig. for comparison. These data by the different investigators have been obtained with quite different experimental geometries from the present one.

It is seen from Fig. 9 that P_s dependence of the present ϕ_e is quite similar to those by Kumada et al and by Sutherland et al. The data plotted do not so differe to each other quantitatively even though the experimental geometries and the cover gas convection patterns were quite different. The maximum deviation between the data by different investigators are about 200%.

The present evaporation rate ϕ_e plotted in Fig. 8 can be expressed by Eq. (1) as function of P_s.

$$\phi_e = 7.01 \times 10^{-3} \; P_s^{1.257} \qquad (1)$$

P_s dependence of ϕ_e as given by Eq. (1) could not be derived from the evaporation theories suggested to date. But, Fig. 8 indicates that the evaporation rate dose not so strongly depend on the pool and the cover geometries.

3. Transient and Steady State Mists Concentration Behavior

For the purpose to investigate mist formation and its coagulation precesses in qualitatively, the transient and steady state mist concentration were measured by the laser concentration meter.

Fig. 10 shows the transient concentration data during gradual pool temperature rising from 335° to 350°C. The concentration increases very sharply at just after the start to heat. After reached the maximum point at 10 minutes after, the concentration begin to decrease. It requires for more than 20 minutes untill attainment of the steady state concentration. As is seen in Fig. 8, the concentration dose not depend on T_s or P_s between the pool temperature range shown in Fig. 10. So, the concentration before and after heating are the same in Fig. 10.

Similar transient data were also obtained with more higher pool temperatures, and the average time required to obtained steady state concentration was about 40 minutes.

At steadty state, there observed the concentration fractuations. The freactuations increase from 2 to 26% as an increase in pool temperature of T_s. The most representative data are shown in Fig. 11, and the maximum fractuation are plotted in Fig. 12.

Two different theories are suggested for sodium mist formation within the cover gas. One is the critical supersaturation model by Epstein et al[6][8], and the other one is the heterogeneous nucleation theory by Kudo et al[9]. Both theories give the initial mist particle sizes of order of 10^{-8} to 10^{-6}cm. Very small particles such as these grow very rapidly to the radius of the order of 0.1 μ m within about 0.1 second, even only by Brownian coagulation[2]. Vapor condesation onto the particles may accelerates the growing rate and this result in more rapid growing.

Such an transient concentration behavior as seen in Fig. 10, which prolonged so long as more than 20 minutes, may not due to coagulation of the very small particles of the order of 10^{-8} to 10^{-6} cm formed at the initial stage of the mist formation.

Coagulation constant of the large particles of the order of 0.1 μ m by Browian motion becomes, at least, two order smaller than that of the above very small particles[5]. So, very slow changing of the concentration shown in Fig. 10 may attributed to coagulation of the large particles. It is also known that the mist particles grow very rapidly to the large sizes of the order of 0.1 μ m within the temperature boundary layer above the pool. Further growing may occure within the main cover gas steam.

Width of fractuations shown in Figs. 11 and 12 have a close correlation with the mist concentration. Because, the concentration increases as an increase in T_s or P_s as seen in Fig. 8, and the fractuation also increase

with T_s or P_s . Coagulation of the mist particles was suggested to be mainly by Brownian motion and gravitational setting, but not by turbulent of the gas[9]. So, the fractuations may occured due to those of the coagulation constant as the results of flow velocity fractuation in gas phase. Figs. 11 and 12 also show that the mist concentration is not always steady state. It changes almost periodicaly with periodic cycles of a few minutes.

4. The Average Mist Particle Sizes.

Sodium mist particle sizes in cover gas space is known to be similar to log-normal distribution[10]. But, for simplicity, it is assumed here in this paper that the particles are monosize.

Under this assumption, gravitational settling velocity V_s of aerosol particle with radius of $\bar{r}$ can be give by Eq. (2).

$$V_s = \frac{2}{9}\frac{\bar{r}^2(\rho_{Na} - \rho_{Ar})g}{\eta}\left(1 + A\frac{\ell}{\bar{r}}\right) \qquad (2)$$

Since, the sodium mist particle radii are known to be the order of a few μ m and are much larger than mean free path ℓ of the cover gas, Cunningham corelation term of $\left(1 + A\frac{\ell}{\bar{r}}\right)$ in Eq. (2) can be regarded to be equal to 1.0.

If the settling mass flux of ϕ_{sett} and the concentration of C are the known quantities, the settling velocity of V_s in Eq. (2) can be derived from Eq. (3).

$$V_s = \frac{\phi_{sett}}{C} \qquad (3)$$

By substituting Eq. (3) into Eq. (2), we obtaine the average particle radius of $\bar{r}$ from the known quantities of ϕ_{sett} and C.

Fig. 13 shows $\bar{r}$ dependence on C thus obtained. Between 0.15 to 2.4 g/m^3 (ie. T_s ; 290°to 420°C) $\bar{r}$ is almost constant with about 6 μ m. Above these, $\bar{r}$ increases from 6 to 13 μ m.

One of the most probable causes of these $\bar{r}$ dependence on C may be the increasse in particle number concentration n as an increase of T_s or P_s. Under the present assumption of monosize particles, the following equation can be used to represent the steady state mist behavior in cover gas.

$$Kn^2 + Rn = \frac{\phi e}{4h} \qquad (4)$$

In this source term in right hand side of Eq. (4) by evaporation of the vapor is independent on number concentration n. But, the removal rate of Rn of the particles is a first order product with n and coagulation probabilities on Kn^2 is a second order product with n. The latter Kn^2 increase remarkably as an increase in n. Therefore, at high mist concentration ranges, n could not be able to increase as an increase in C, because rapid growing and followed rapid disappearance of the particles may occure by the gravitational settling. Fig. 14 shows this. The present number concentration n is plotted as a function of C under monosize assumption. It is seen in Fig. 14 that n increases as an increase in C up to about 2.2 g/m^3 at T_s of 420°C. But, it becomes almost constant above this.

In addition to above mentioned $\bar{r}$ determination, the determination by means of the laser concentration meter was also carried out. This is for obtaining the smaller side of the particles. Experimental method for this is that, prior to the measurements, the pool sodium was drained after sufficient steady state operation with T_s of about 450° to 500°C.

After draining, trace heaters of the test vessel were turned off and dense mists were allowed to settle and deposit for about 10 hours. When the temperature of the vessel was lowered down to about 100°C homogeneously around the vessel and the concentration became dilute enough so that the particles removaling was mainly by gravitiational settling, the measurements of the concentration decay have been carried out. From

the measured decay curve, the average particle size of the mist were calculated from Eq. (2).

Since the large particles have been already settled down at the time of the measurements, $\bar{r}$ derived by this method may present the smaller side radius of the mists than mass mean radius. In addition, thus obtained data may not so differe by the pool temperatures. Because, the average radius dose not so strongly depend on T_s as seen in Fig. 12 and the difference is about twice.

Fig. 15 shows $\bar{r}$ data derived by this mentioned and those which were derived by the early mentioned settling mass flux and concentration measurements. The $\bar{r}$ derived by the latter method may gives the larger side radius than mean mass, since these data were derived from the gravitational settling flux. In Fig. 15, the data published in ANL report[10] are also plotted for comparison with the present data. ANL data were reported to be determined by using of cascade impactor at the pool temperature of 400°C, but not reported the experimental geometry. Their data agree well to the present ones. It could be said from Fig. 15 that the mist particle radius is between 1.5 to 15 μ m under the pool temperature range of 350° to 520 °C.

IV. Conclusions

For the purpose to investigate the pool temperature dependence of the sodium mist concentration, the mist particle sizes and evaporation rate of the vapor, the experiment was carried out by using of a cylindrical test vessel of 305.5 mm I.D and 1,800 mm in length. Cover gas space above the pool is about 1,400 mm in length and about 100 ℓ in volume.

The experimental results are summarized as follows.

1 The concentration is a function of the saturated vapor pressure of P_s at the pool surface. It is 0.15 to 15 g/m^3 between the pool temperature of T_s of 350° to 520°C. The temperature dependence of the concentration changes at 290°, 350° and 420°C.

2 The evaporation rate derived by the gravitational mists settling flux data is only a function of P_s above T_s of 400°C. It was estimated that the rate dose not so strongly depend on pool and cover gas geometries.

3 When the pool temperature changed, the concentration changes transiently for 20 to 40 minutes. At steady state, the concentration fractuates for about 2 to 26% as an increase in T_s between 310° to 450°C, and the fractuation is almost periodicaly.

It was estimated from the data that the mist behavior in cover gas is controlled by coagulation of the large particles of the order of 0.1 μm radius. But, not by that of the very small particles formed at the initial stage of the mist formation.

4 The mist particle radius is between 1.5 to 15 μm between T_s of 350° to 520°C.

Aknowledgements

The authors express their deep gratitude to Mr. R. Saito, Manager of Sodium Engineering Division of PNC and Dr. E. Ishibashi of O-ita University for their continuous encouragements and advices throughout the work. The technical arrangement given by Dr. K. Mochizuki and Mr. K. Yamamoto of PNC Head Office, the technical suggestions given by Dr. G. Nishio of JAERI and Dr. K. Takami of Hitachi Central Recearch Laboratory for designing of the laser concentration meter, and the technical assistance of Mr. Y. Hashimoto of PNC in conduction of the experiments were also greately acknowledged.

Nomenclatures

d ; pool diamter (cm)

C ; mist concentration (g/cm^3 or g/m^3)

h ; cover gas hight (cm)

K ; mist coagulation constant (ℓ/sec)

ℓ ; pean free path (cm)

P_s ; satuaated vapor pressure or the pool surface (atm)

R ; mist removal rate (1/sec)

T_s ; pool temperature (^oC)

r ; mist radius (μm)

$\bar{r}$; average mist radius (μm)

ϕ_{sett} ; mists settling mass flux (g/cm^2. sec)

ϕ_e ; evaporation rate of the vapor (g/cm^2. sec)

ρ_{Na} ; Na density (g/cm^3)

ρ_{Ar} ; Argon density (g/cm^3)

η ; viscosity (g/cm. sec)

λ ; wave length (μm)

α ; particle size parameter ($=\frac{2\pi \bar{r}}{\lambda}$)

η ; trap efficiency (%)

References

(1) Himeno, Y. et al.: to be published

(2) Spiegler, P., et al.:"Evaluation of The Equation That Governs The Coagulation of An Aerosol", Pcor. 9th AEC Air Cleaning Conf., Boston. 1976. CONF-660904. Vol I, II. 629-646.

(3) Lauben, G. N., et al. : "Characterisation of Source Terms for Aerosol Transport During Sodium Fires" , ibit.

(4) Roth, C., et al.: "Size Spectrometry of Submicron-Aerosol by Counting Single Particles Illuminated by Laser Light", J.of Colloid and Interface Science . 54 . No. 2,265-277. Feg. 1976.

(5) Takahashi, K.: "Kiso Aerosol Kogaku". (in Japanese) Yokendo. 1972.

(6) Kumada, T., Kasahara, F and Ishiguro, R.: J. Nucl. Sci. Technol, 13 . No.2, 74-80. 1976.
Kumada, T, Abe, T and Ishiguro, R.: (in Japanese). Bull. of JSME , 43 . No. 370. 2278. 1976.

(7) Sutheland, J.D., et al.: Trans ASME , Series A. 92-4. 1970.

(8) Epstein, M and Rosenter, D.M.: Int.J.Heat Mass Transfer, 13 439. 1970.

(9) Kudo, K and Hirata, K.: (in Japanese). Bull. of JSME, 42 No. 361. 2900. 1976.

(10) ANL Report.: ANL-ST-4, Sept., 1970.

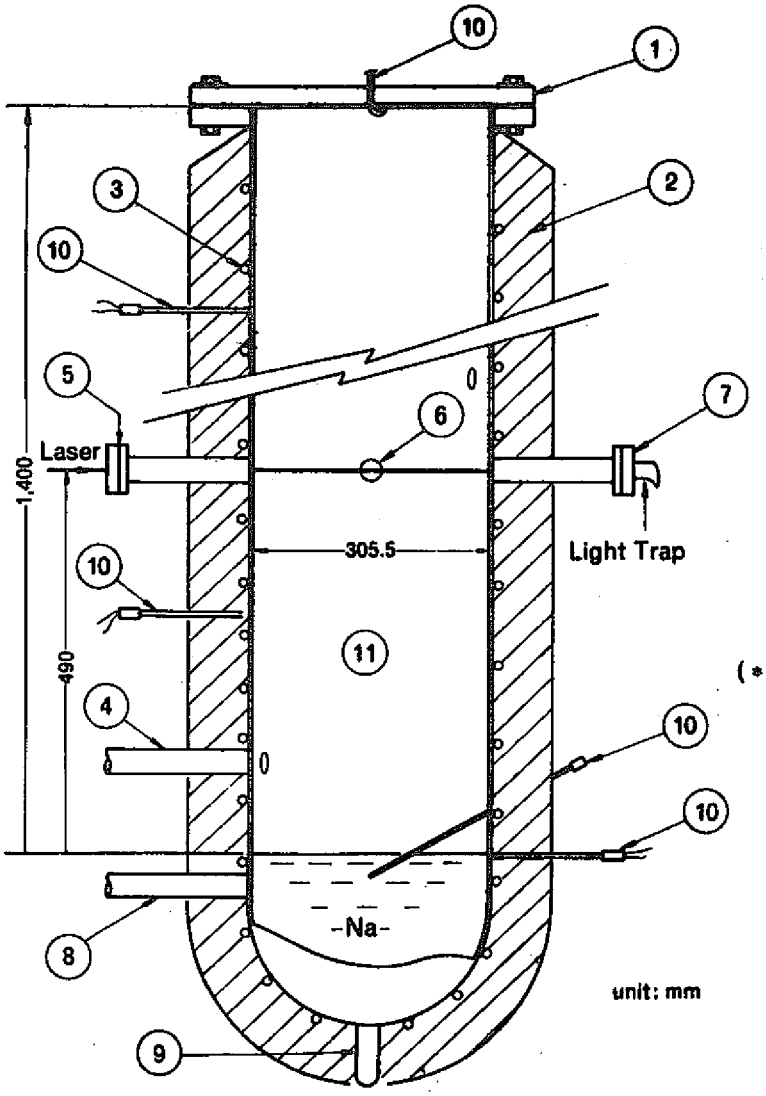

① Top Flange
② Thermal Insulator
③ Trace Heater
④ Gas Piping
⑤ Laser Window (for Primary Beam)
⑥ Hole for Laser Window(*) (for Scattered Beam)
⑦ Laser Window (for Outgoing Beam)
⑧ Na Outlet
⑨ Na Inlet
⑩ Thermocouple
⑪ Argon Cover Gas Space

(*) ⑥ was also used for ϕ_{sett} determination

Fig. 1 Test Vessel

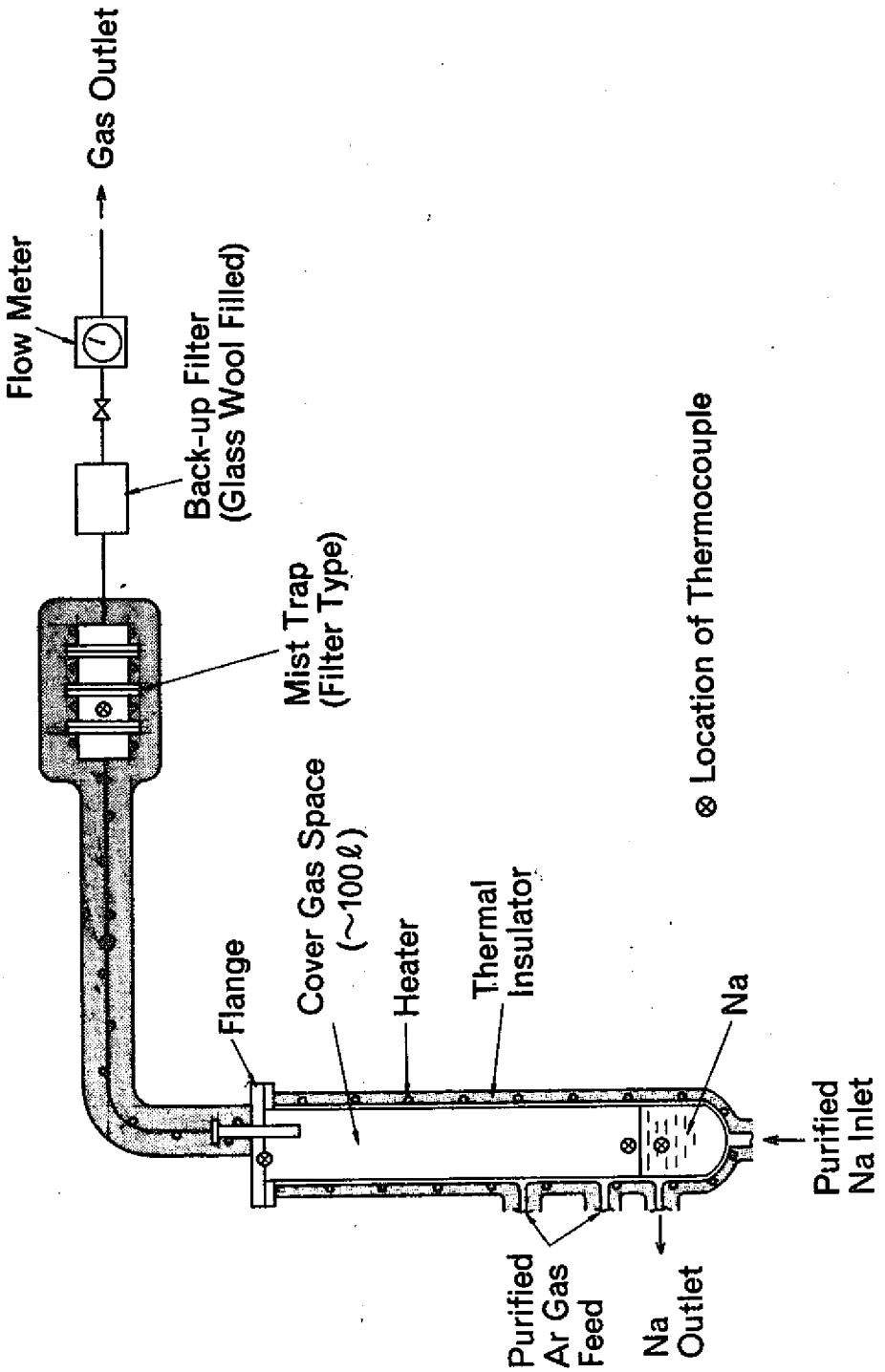

Fig.2 Experimental Arrangement for Mist Collection(Ⅰ)

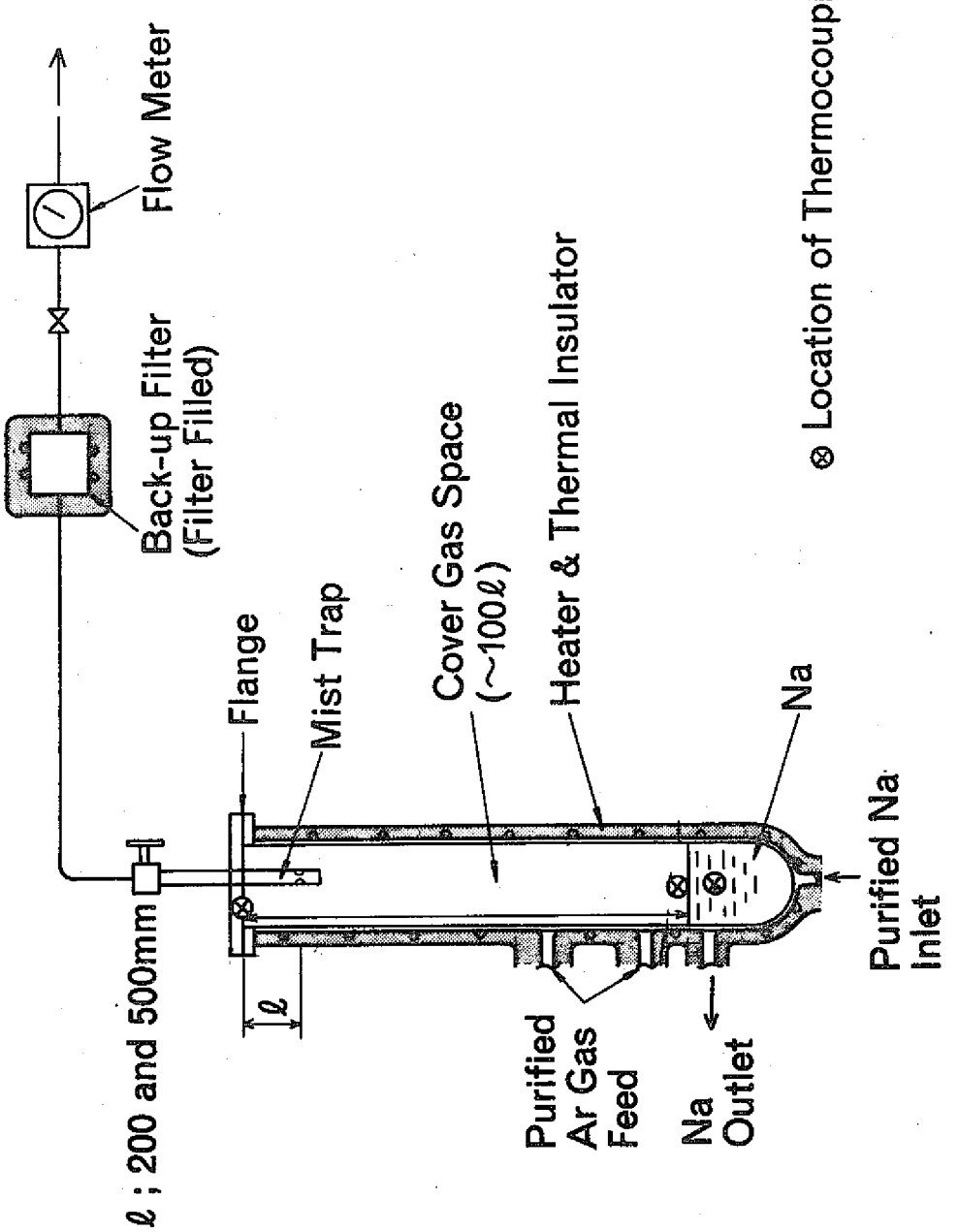

Fig. 3 Experimental Arrangement for Mist Collection (II)

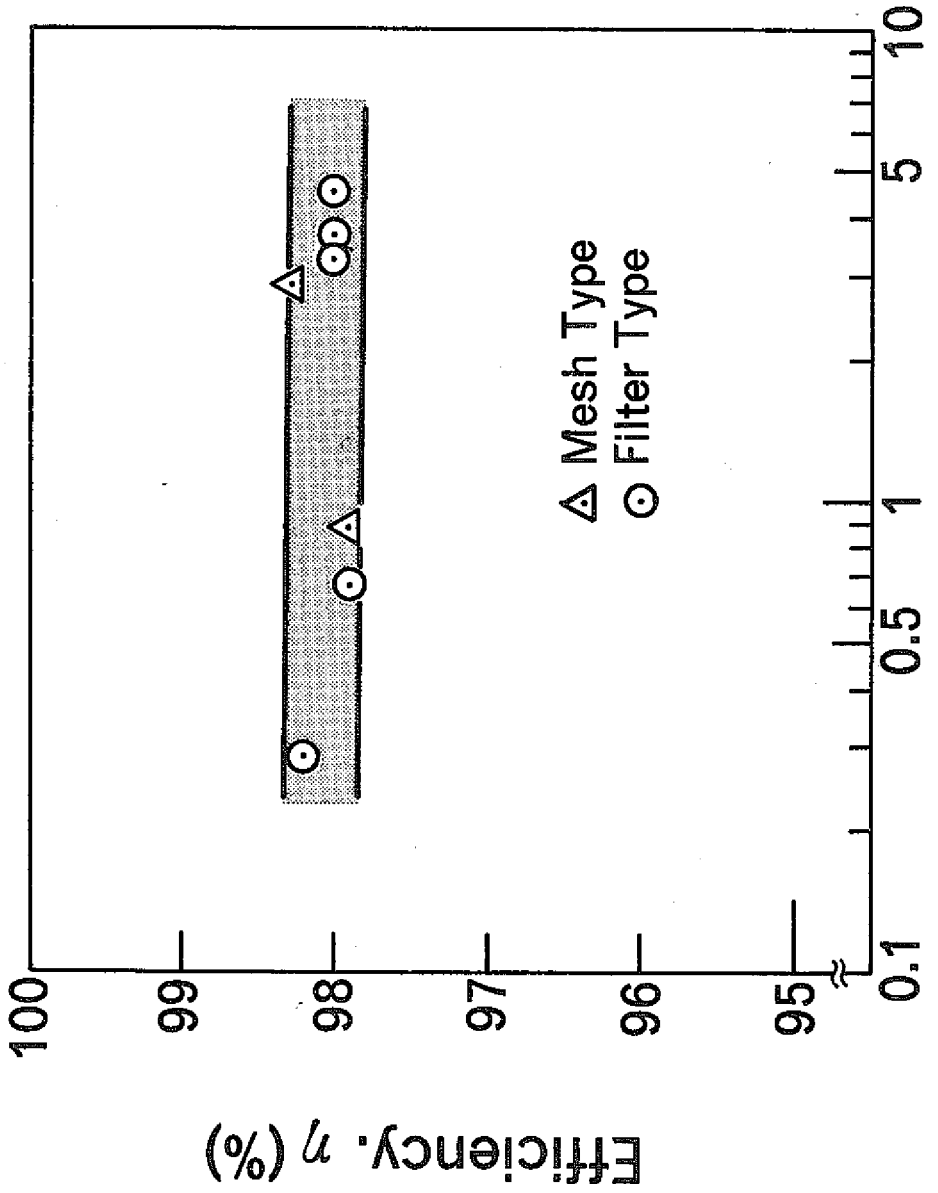

Fig. 4 Efficiency of Mist Traps

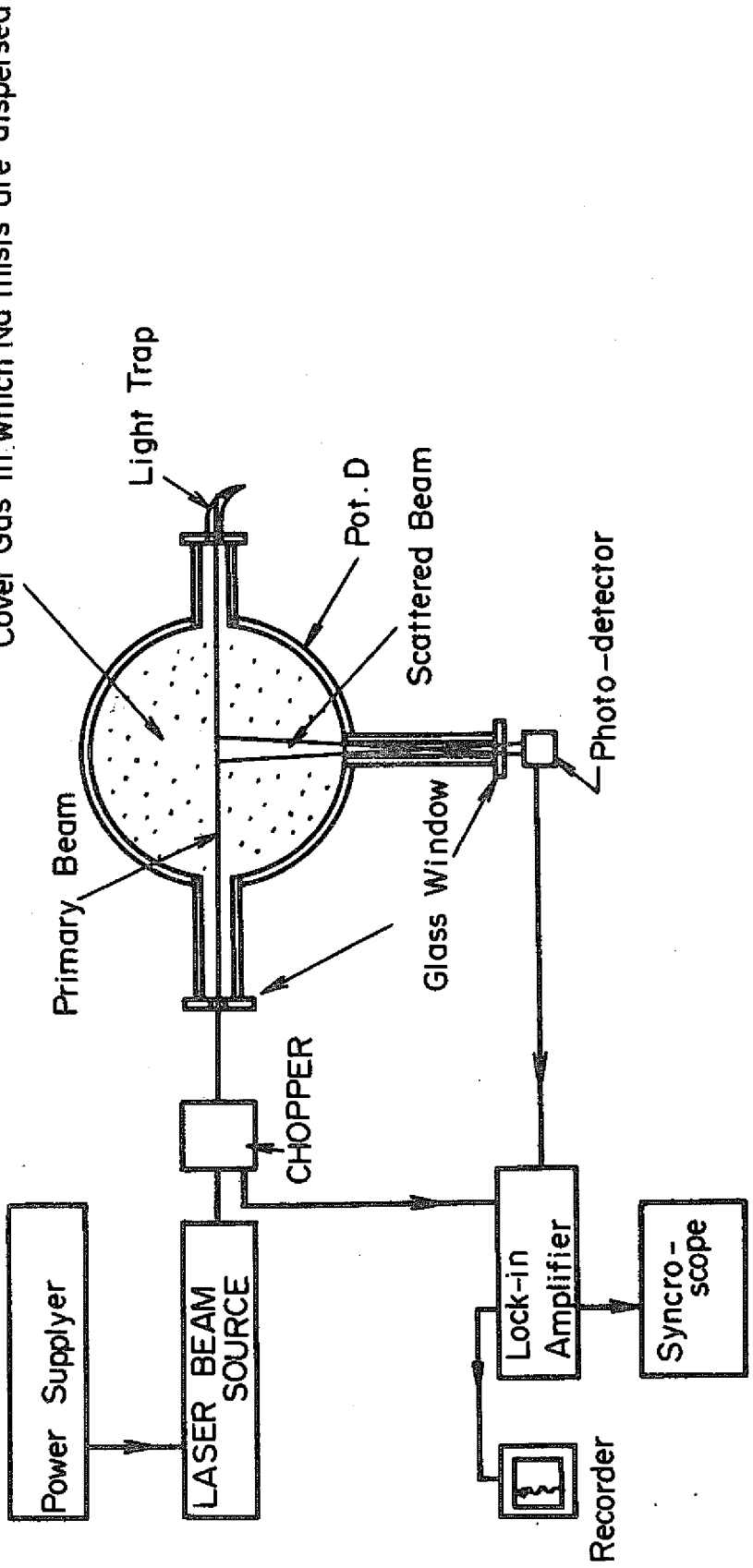

Fig. 5 Arrangement of the Mists Concentration Meter (Cross-sectional View)

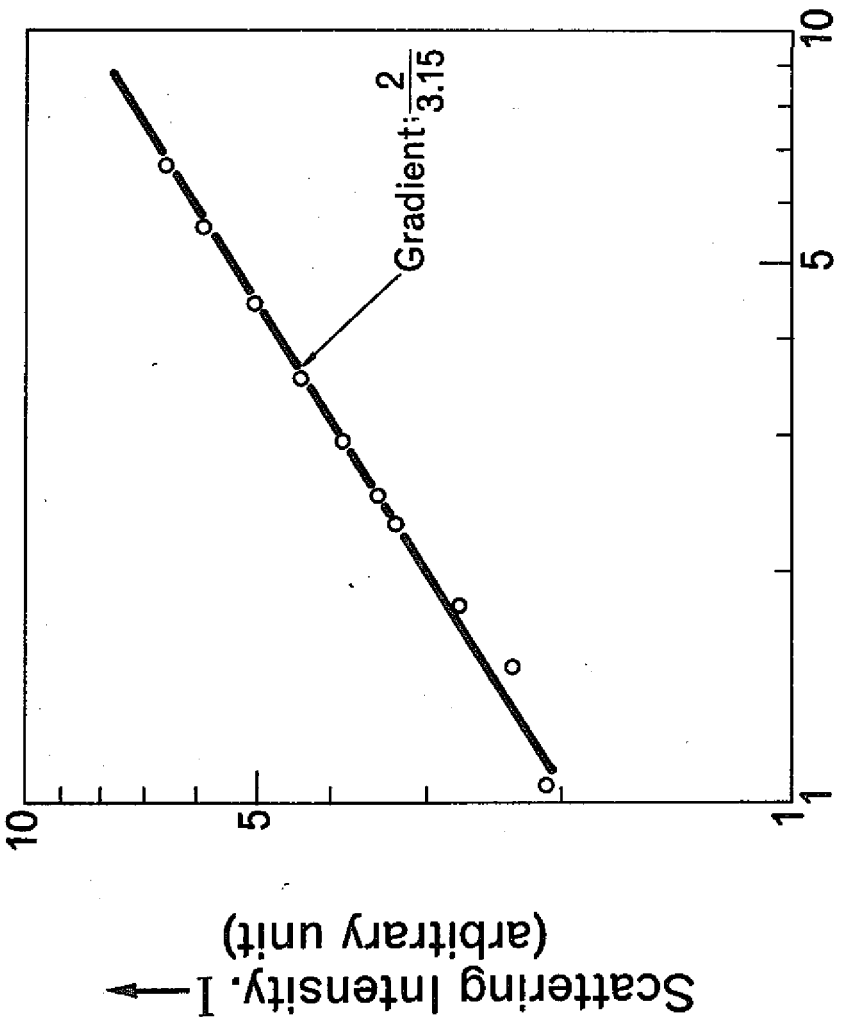

Fig. 6 Intensity of Scattered Laser Beam as a Function of Mass Concentration

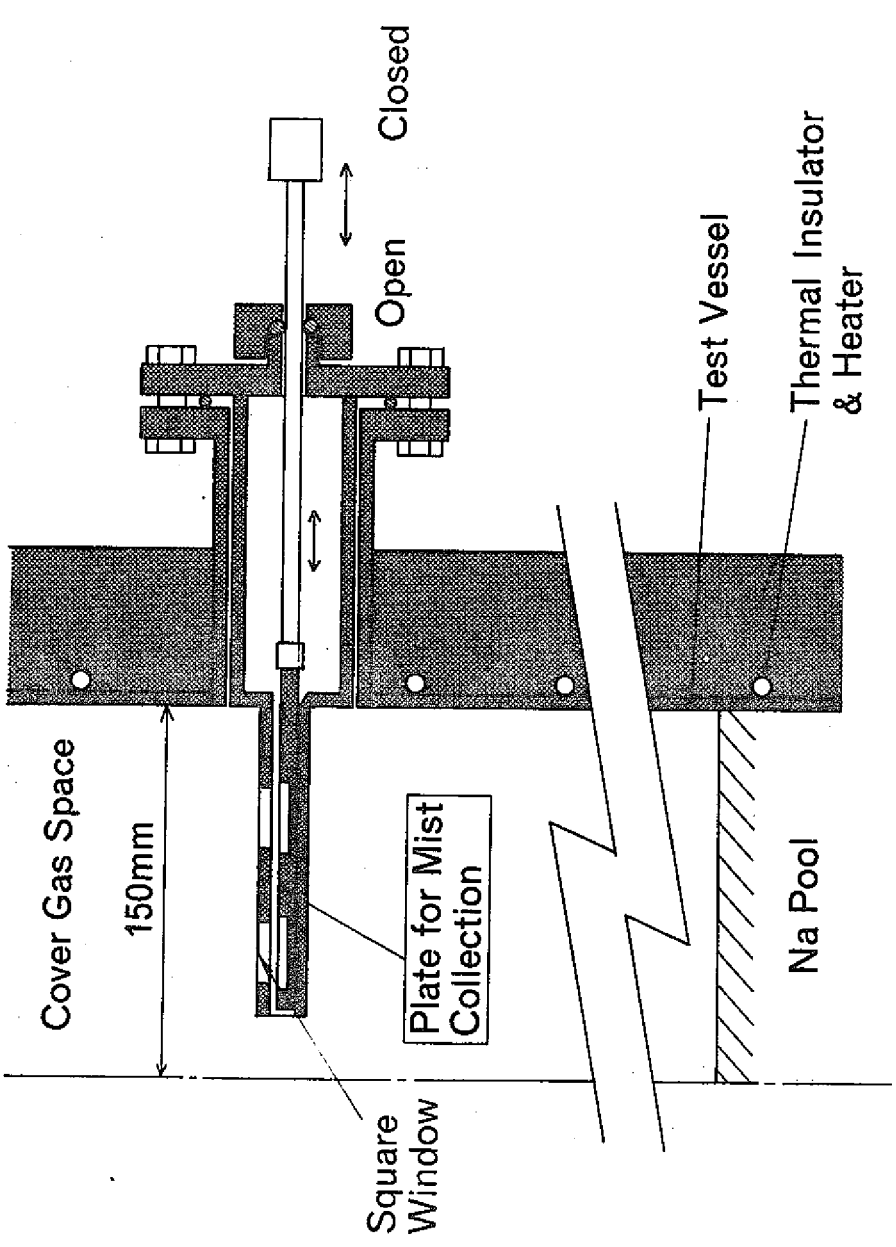

Fig. 7 Arrangement of the Device for Settling Mass Flux Measurement

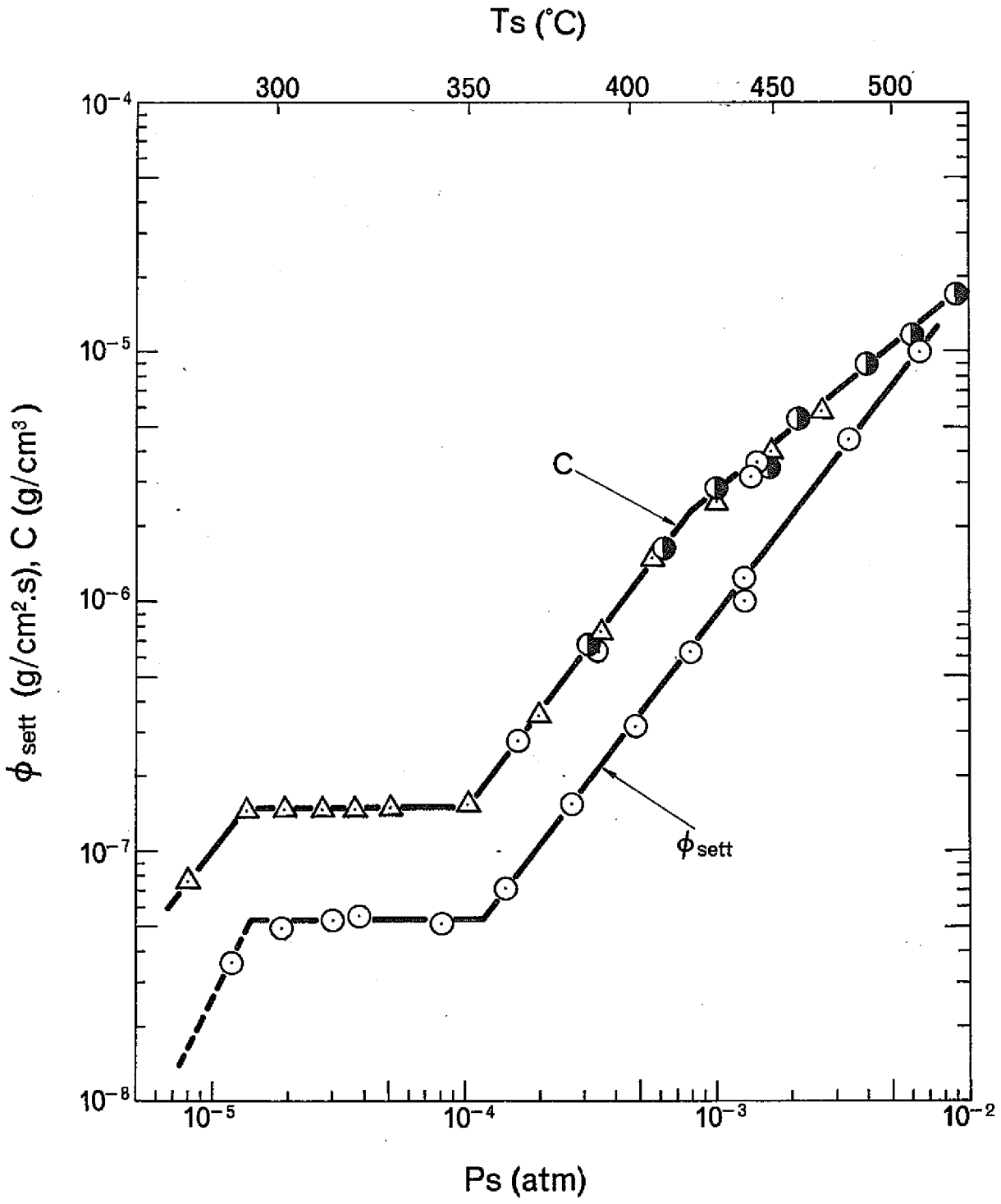

Fig. 8 Mass Concentration C and Settling Mass Flux ϕ_{sett}

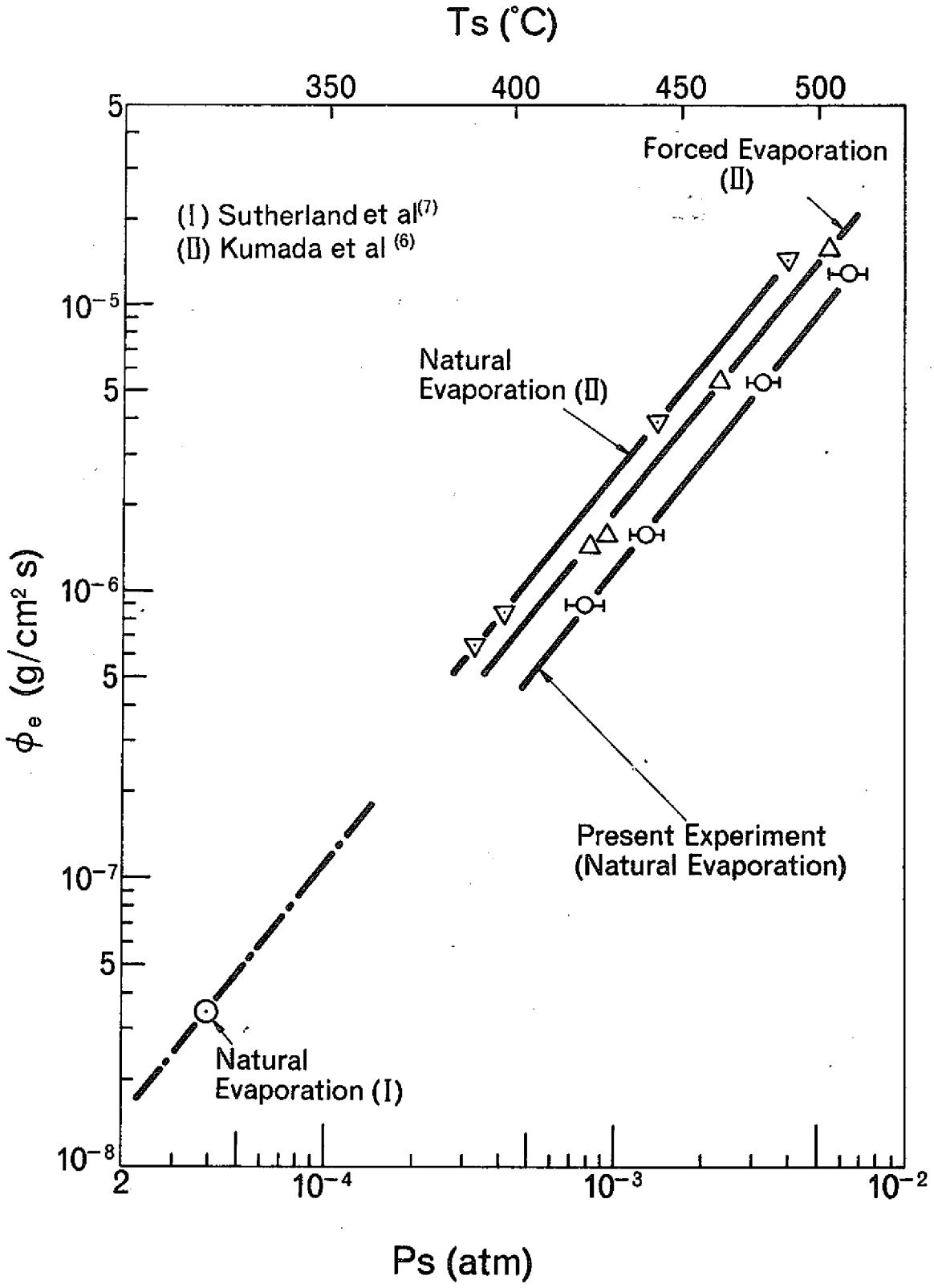

Fig. 9 Experimental Evaporation Rates

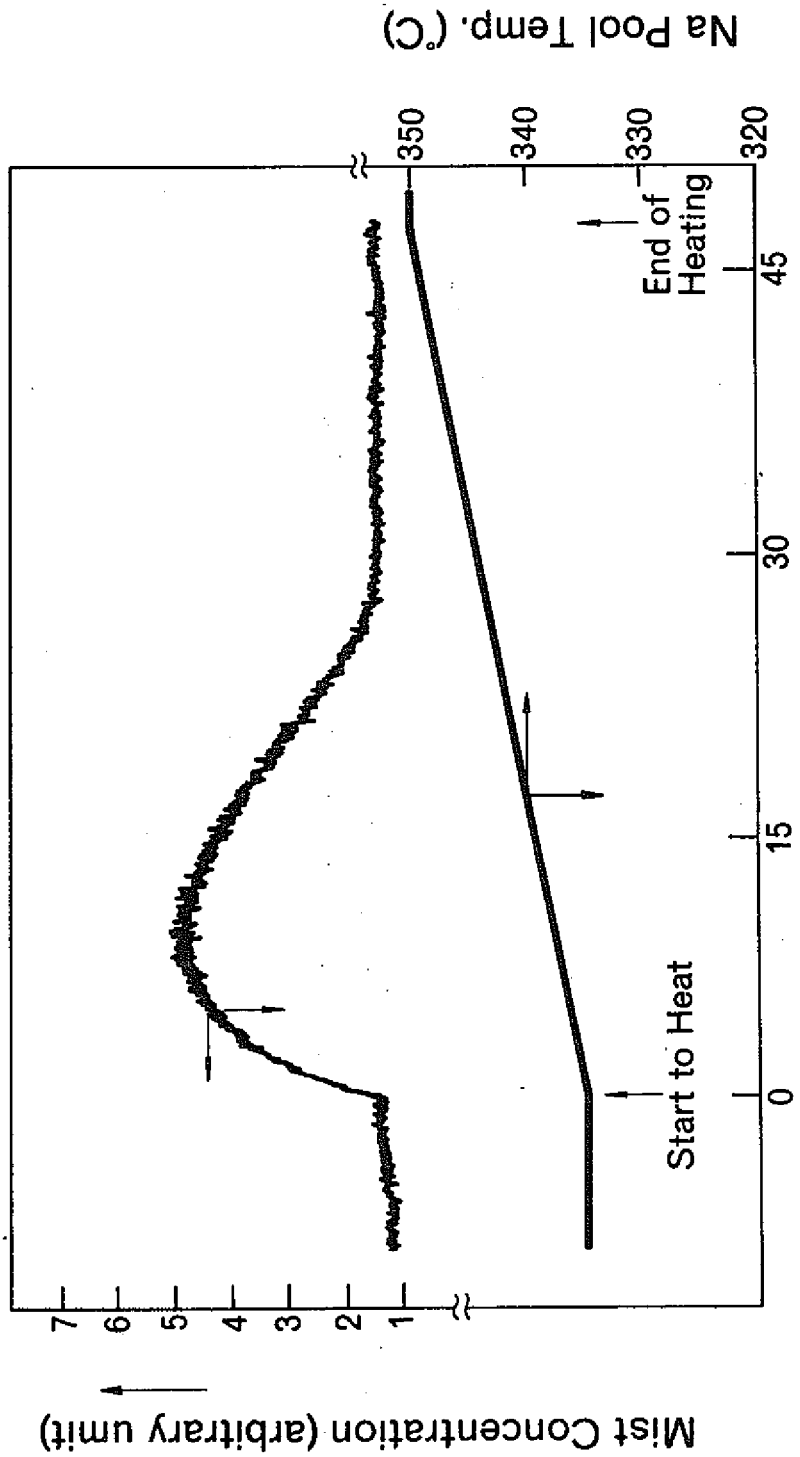

Fig. 10 Transient Mist Concentration Change During Na Pool Temperature Rising (By Laser Concentration Meter)

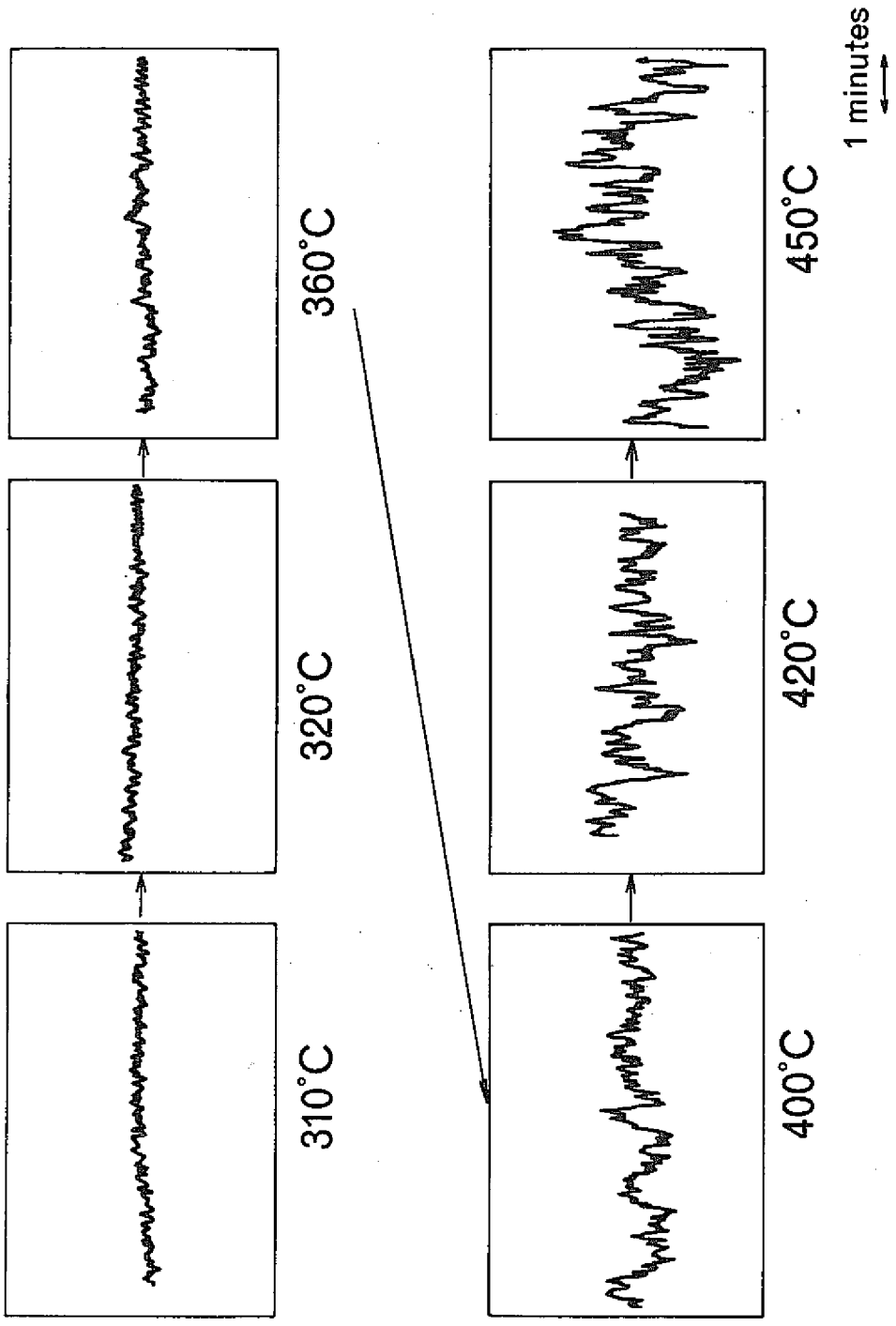

Fig. 11 Fractuation in Mist Concentration as a Parameter of Pool Temperature Ts

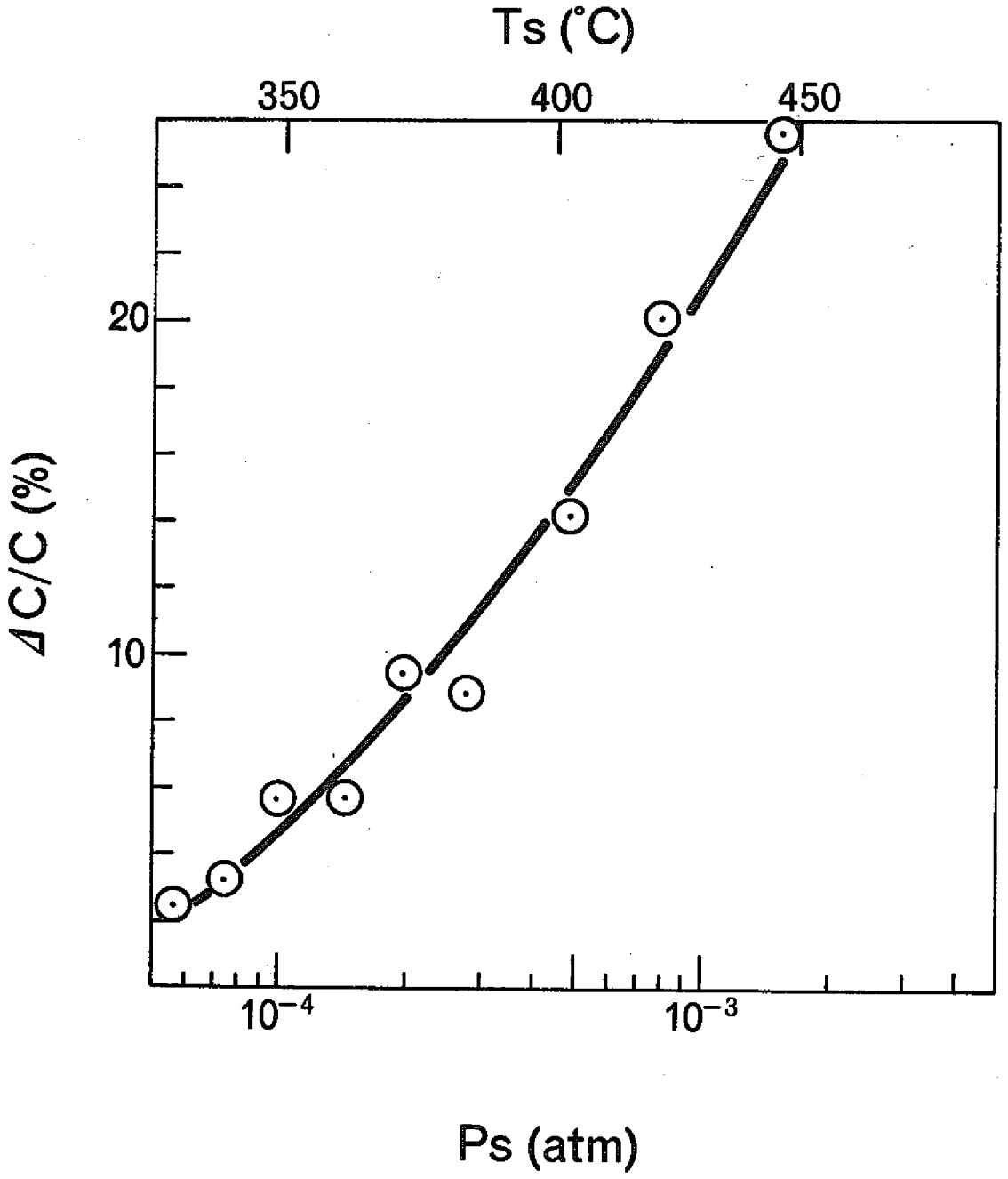

Fig. 12 The Maximum Concentration Fractuation at Steady State

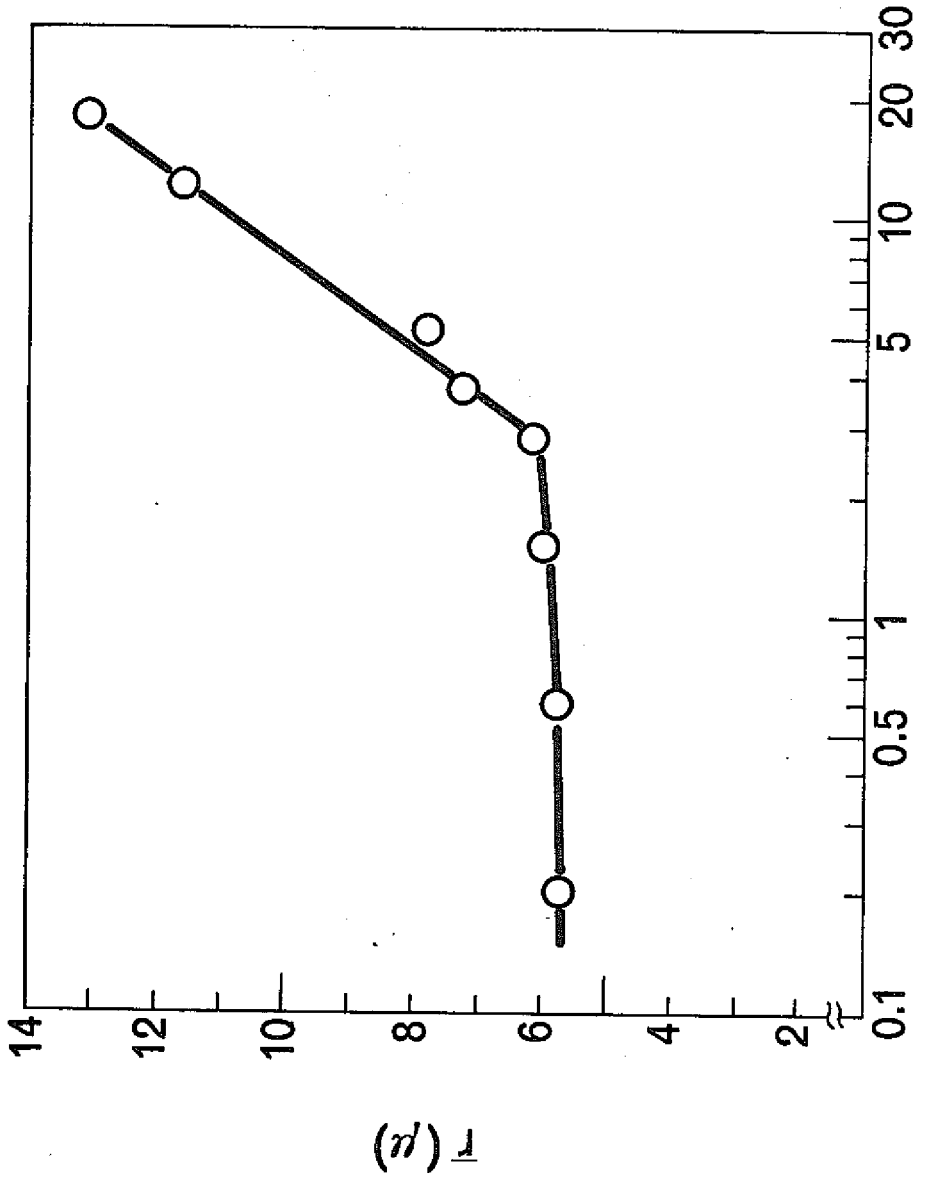

Fig. 13 Average Mist Particle Radius as a Function of Concentration

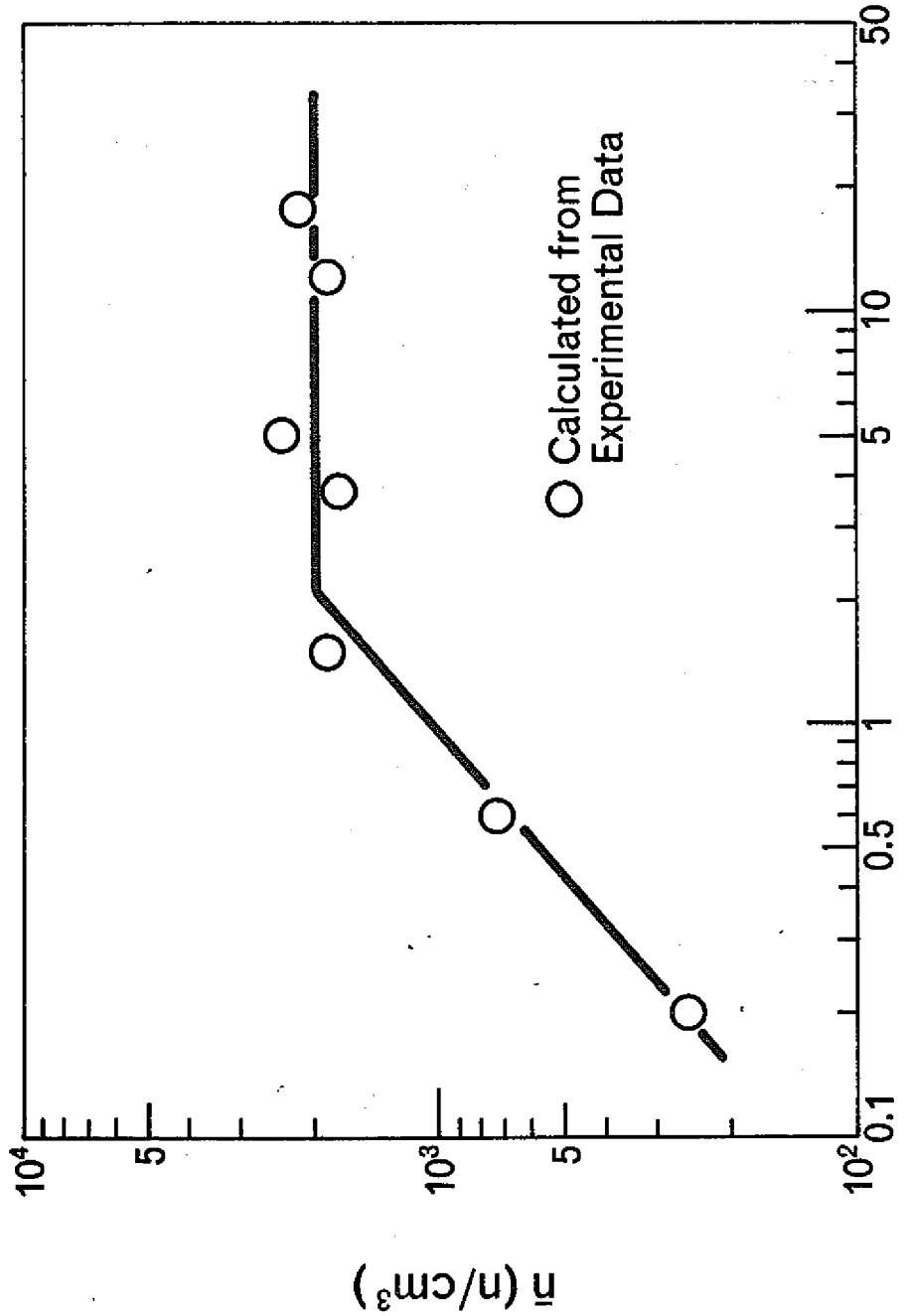

Fig. 14 Number Concentration of Mist Particles as a Function of Mass Concentration C

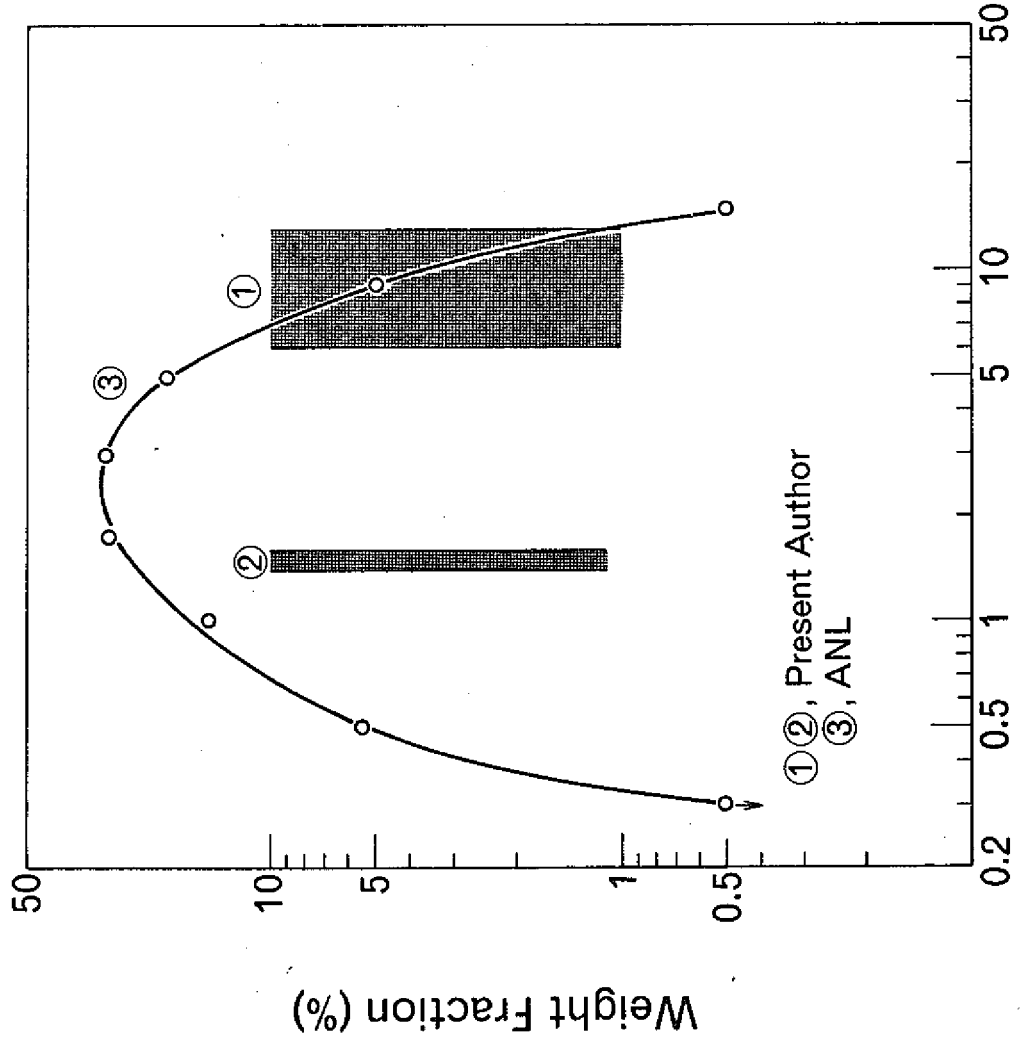

Fig. 15 Experimental Sodium Mist Particle Sizes